

## MHD Flow Layer Formation in Vicinities of Rational Flux Surfaces of Tokamak Plasmas

J. Q. Dong, Y. X. Long, Z. Z. Mou, and J. Q. Li  
Southwestern Institute of Physics, P. O. Box 432 Chengdu, China  
e-mail contact of main author: jiaqi@swip.ac.cn

**Abstract** Linear and quasi-linear development of double tearing modes induced by electron viscosity and plasma resistivity in plasmas of reversed magnetic shear is numerically analyzed. The spatio-temporal characteristics of the magnetic configuration and plasma velocity are studied in detail. MHD flow layers are demonstrated to merge in the development of the modes. The sheared flows are shown to lie just at the rational surfaces in the linear stage and at the boundaries of the magnetic islands in the quasi-linear stage. The flows have sufficient levels of shear required for turbulence suppression. Possible correlation between the layer formation and triggering of experimentally observed internal transport barriers, preferentially formed in vicinities of rational flux surfaces of low safety factors, is discussed.

### 1. Introduction

Advanced operation modes with external and internal transport barriers (ETBs and ITBs) are desirable for magnetic fusion ignition in toroidal devices such as tokamaks and stellarators. Therefore, ITB formation mechanism is an important topic of magnetic fusion plasma physics and has attracted much attention in recent years. The ITBs are often found to form in vicinities of low safety factor  $q$  rational flux surfaces in discharges with monotonic as well as non-monotonic  $q$  profiles and to coincide with MHD activities in experiments [1,2]. On the other hand, the crucial role of sheared flows in formation of ETBs and ITBs in advanced tokamak discharges has been demonstrated in recent decades. [3]. Two kinds of flows have essentially been considered: mean flow and zonal flow of  $m=n=0$ . Here,  $m$  and  $n$  are poloidal and toroidal mode numbers of the flows, respectively. The mean flows are created by outside sources such as neutral beam injection, radio frequency wave launching and biased voltage application etc., or by variation of plasma equilibrium parameters. The zonal flows emerge from nonlinear coupling of turbulent fluctuations. The suppression effects of the mean flows on turbulent fluctuation, resulting in confinement improvement, are well documented. In addition, theories and simulations indicate that plasma mass, velocity and energy diffusions across magnetic flux surfaces may be regulated by zonal flows in absence of mean flows. Nevertheless, neither the mean nor zonal flows are necessary to form near rational surfaces and theory on creation mechanisms of the flows at the positions and time, especially, of ITB formation is still a lack.

A third kind of flow--MHD flow may exist in tokamak plasmas and is studied in this work. The characteristics of the MHD flows may be summaries as: 1) driven by magnetic energy released in MHD activities, 2) with helical structures, 3) large spatial scales and 4) slow temporal scales in comparison with turbulence.

It is well known that low order rational flux surfaces are prone to excitation of ideal and dissipative MHD instabilities and that magnetic energy released in the development of the modes may drive significant plasma flows. In particular, very localized flows have been found in linear and non-linear development of resistive tearing modes in tokamak plasmas [4,5]. In linear stage, Ishii *et al.* and Held *et al.* found very sharp structures of the velocity stream functions at the rational surfaces (See Figures 3 and 4 of Ref. 4 and Figure 5 of Ref. 5), indicating that there were velocity layers at these positions. In non-linear stage, the same authors discovered that helical and poloidal flow layers were created around the magnetic islands (See Figure 11 of Ref. 4 and Figure 16 of Ref. 5).

In the Large Helical Device (LHD), simulations have shown that helical sheared flow layers were formed near the boundaries of the magnetic islands induced by nonlinear development of interchange modes [6]. In addition, poloidal velocity layers at the boundaries of the magnetic island resulted from external helical currents were observed in experiments [7]. The amplitude of the velocity was found to increase with the width of the magnetic islands.

All these flows have the characteristics of MHD flow defined above.

Quantitative study of the MHD flow layer formation mechanism and of possible correlation between the flows and turbulence is at its initiative stage [8,9] although qualitative evidences are clear. The features of double tearing mode that develops in plasmas of double resonant surface with shear reversed safety factor  $q$  profiles have been studied systematically and the results are summarized in this work. The characteristics in the initial development stage of the mode mediated by anomalous electron viscosity studied in previous works [8,9] are briefly reviewed first. Then, the full development of the modes mediated by electron viscosity as well as plasma resistivity is presented in detail. The emphasis is placed on the creation of sizable sheared MHD flow layers at the boundaries of the magnetic islands created in the development of double tearing mode mediated by plasma resistivity.

The remainder of this work is organized as follows. The physics model and equations are presented in Section 2. The numerical results are described in Section 3. Section 4 is devoted to conclusions and discussion.

## 2. Physical Model and Basic Equations

A typical sheared slab of scale length  $a$  in the  $x$ -direction, with a current in the  $z$ -direction, and zero equilibrium flow velocity  $\mathbf{V}_0=0$  embedded in the standard sheared magnetic field is employed,

$$\mathbf{B}_0(x) = B_{0y}(x)\hat{y} + B_{0z}(x)\hat{z}$$

where  $B_{0y}(x)$  equals zero at the two rational surfaces  $x=\pm x_s$ . The stability of this initial configuration will be examined with respect to two-dimensional, incompressible perturbations. The vector fields are expressible in terms of two scalar potentials : the flux function  $\psi$  and the velocity stream function  $\phi$  [8,9] . Spectrum method is adopted

for the potentials and the quasi-linear equations for the zeroth and the first harmonics of  $\psi$  and  $\phi$  are,

$$\begin{aligned}\frac{\partial \delta \psi}{\partial t} &= -\frac{k}{2} \left( \frac{\partial \bar{\phi}_1}{\partial x} \bar{\psi}_1 + \bar{\phi}_1 \frac{\partial \bar{\psi}_1}{\partial x} \right) + \frac{1}{S} \left( \frac{d^2 \psi_0}{dx^2} + \frac{\partial^2 \delta \psi}{\partial x^2} \right) - \frac{1}{R} \left( \frac{d^4 \psi_0}{dx^4} + \frac{\partial^4 \delta \psi}{\partial x^4} \right) + E', \\ \frac{\partial \bar{\psi}_1}{\partial t} &= -k \bar{\phi}_1 \left( \frac{d \psi_0}{dx} + \frac{\partial \delta \psi}{\partial x} \right) + \frac{1}{S} \left( \frac{\partial^2 \bar{\psi}_1}{\partial x^2} - k^2 \bar{\psi}_1 \right) - \frac{1}{R} \left( \frac{\partial^4 \bar{\psi}_1}{\partial x^4} - 2k^2 \frac{\partial^2 \bar{\psi}_1}{\partial x^2} + k^4 \bar{\psi}_1 \right) \\ \frac{\partial}{\partial t} \left( \frac{\partial^2 \bar{\phi}_1}{\partial x^2} - k^2 \bar{\phi}_1 \right) &= k \left( \frac{d \psi_0}{dx} + \frac{\partial \delta \psi}{\partial x} \right) \left( \frac{\partial^2 \bar{\psi}_1}{\partial x^2} - k^2 \bar{\psi}_1 \right) - k \left( \frac{d^3 \psi_0}{dx^3} + \frac{\partial^3 \delta \psi}{\partial x^3} \right) \bar{\psi}_1 \\ &\quad + \frac{1}{R_i} \left( \frac{\partial^4 \bar{\phi}_1}{\partial x^4} - 2k^2 \frac{\partial^2 \bar{\phi}_1}{\partial x^2} + k^4 \bar{\phi}_1 \right)\end{aligned}$$

where,  $R = \tau_v / \tau_h$  is the electron dynamic Reynolds number,  $\tau_v = \omega_{pe} a^4 / c^2 \mu_e$  is the electron viscosity decay time,  $S = \tau_r / \tau_h$  is the magnetic Reynolds number,  $\tau_h = a / v_A$  is the Alfvén time with  $v_A$  being the poloidal Alfvén velocity, while  $\tau_R = 4\pi a^2 / \eta c^2$  is the resistivity decay time.  $\mu_e$  and  $\eta$  are electron viscosity and plasma resistivity, respectively.  $\psi_0$  is the equilibrium flux function.

Such a truncating as employed above may introduce unexpected errors. However, our new results with finite difference technique in both the  $x$  and  $y$  directions (not shown in this work and will appear in a separate work soon) indicate that the essential conclusions of this work are not influenced except that the process leading to full reconnection is different due to effects introduced by nonlinear interaction between harmonics.

### 3. Numerical Results

For the magnetic field, we employ the configuration used in Ref. 8. The resistivity and the viscosity are both assumed to be constant. The chosen parameters are  $k=0.25$ ,  $R=10^5$ ,  $S=9.4 \times 10^5$ , and two rational flux surfaces at  $x = x_s = \pm 0.25$ , unless otherwise stated. The results are checked to be independent of the box boundary, the grid size and the time-step. Total 1001 grid points are used in the simulation domain  $[-4, +4]$  and time-step is  $5 \times 10^{-4}$  for the results given below. The effects of the resistivity are negligible and the instability is fully induced by the electron viscosity for above parameters.

The magnetic energy (including the energy of the equilibrium and perturbed magnetic fields)

$$E_m = \frac{1}{8\pi} \int (B_x^2 + B_y^2) dx dy = \int \frac{1}{8\pi} [(k \bar{\psi}_1 \sin ky)^2 + \left( \frac{\partial \psi}{\partial x} \right)^2] dx dy$$

and the kinetic energy

$$E_k = \frac{1}{8\pi} \int (v_x^2 + v_y^2) dx dy = \frac{1}{8\pi} \int [(k\bar{\phi}_1 \cos ky)^2 + (\frac{\partial \bar{\phi}_1}{\partial x} \sin ky)^2] dx dy$$

as functions of time are given in Figs.1(a) and (b) for  $x_s=0.25$  double tearing case. Here, the magnetic field is normalized to  $B_{0y}(\pm \infty)$ , while in the final expression of  $E_k$  the velocities are measured in units of the poloidal Alfvén velocity. It is clearly shown that the magnetic energy released in the reconnection process converts to kinetic energy and can drive large flows in the first stage of the mode development. Then the energy bounces back and forth between magnetic and kinetic for a couple of times with decaying amplitudes and finally goes into a stage when both the kinetic and magnetic energy keep approximately constant. The perturbed magnetic energy in harmonics  $m=0$  and  $1$  (i.e., the components relevant to  $\delta\psi$  and  $\bar{\psi}_1$ , respectively) as functions of time is given in Fig.1(c). It is clearly shown that the magnetic energy in harmonic  $m=1$ , is higher than that in the harmonic  $m=0$  for  $t \leq 40$  that is the linear development stage. The latter grows rather fast after  $t \sim 60$  and dramatically exceeds the former later. This is reasonable since the harmonic  $m=0$  represents the major non-linear effects that is negligibly small at the linear stage and grows dramatically at the quasi-linear stage in the system studied here.

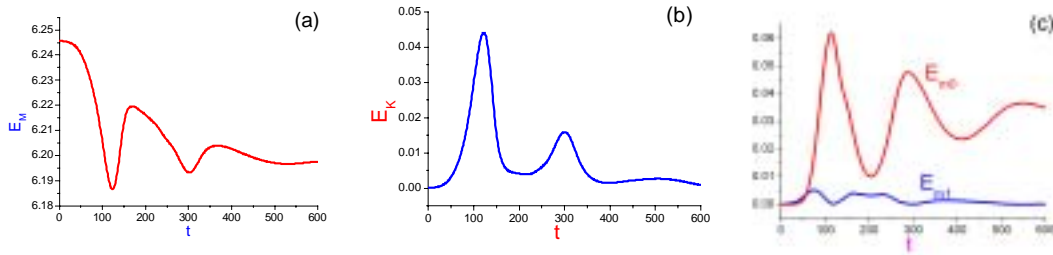


Fig.1, The (a) magnetic energy  $E_m$ , (b) kinetic energy  $E_k$ , and (c) energy in harmonics  $m=0$  and  $m=1$ ,  $E_{m0}$  and  $E_{m1}$ , versus time.

Shown in Fig. 2(a) are the profiles of  $B_x$  (the line in purple) and  $d\bar{v}_y/dx$  (the line in red) at  $t=100$ . It is clearly demonstrated that there is noticeable value of velocity shear at the boundaries of the magnetic islands, where the radial component of the magnetic field  $B_x$  approaches zero. This point will be discussed again later. From the expressions for the magnetic field, the plasma velocity, and the perturbation potentials, Eqs.(1-2) and (7-8),

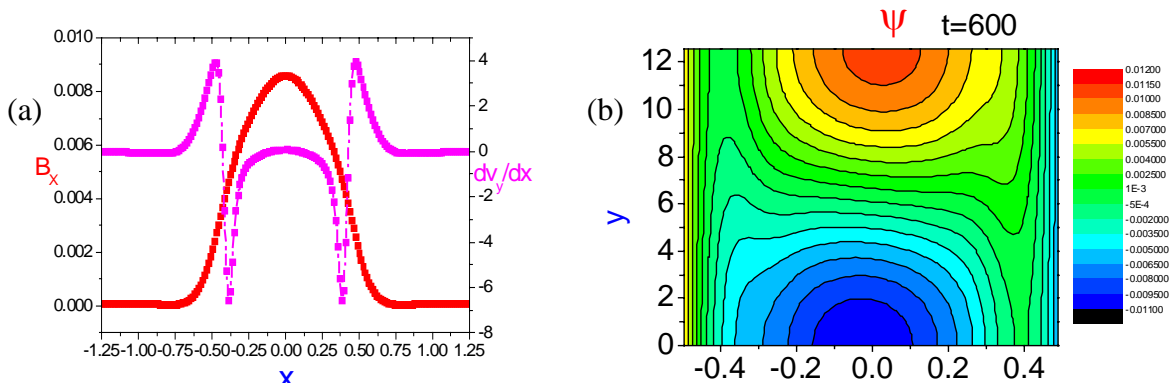


Fig.2 The profiles of  $B_x$  and  $d\bar{v}_y/dx$  (a) and the structure of the magnetic islands (b) at  $t=600$ .

we note that the maxima of the velocity  $v_y$ , its shear  $d\bar{v}_y/dx$ , the radial component of the magnetic shear  $B_x$  and its gradient  $dB_x/dx$  appear at same position in the  $y$ -direction. It is located at the center between the two o-points of the two magnetic islands.

Shown in Fig.~3 are the profiles of  $B_{y0}(x)$  including both the equilibrium  $\psi_0$  and  $\delta\psi$  induced components at  $t=0, 100, 200, 400$  and  $600$ . There are two resonant surfaces,  $B_{y0}(x)=0$ , at  $x=\pm 0.25$  at  $t=0$ . Late, the profile evolves complicatedly as the tearing mode develops and reaches a shape where there are no resonant surfaces, approaching full reconnection, finally. This is a simplified reconnection process and may not be true in a real system there are plasma heating and thermal transport that contribute to the evolution of the equilibrium configuration. However, this clearly show the reason for the evolution of energy partition presented in Figure 1(c) where the major perturbation of the magnetic energy is shown to be in the  $m=0$  harmonics.

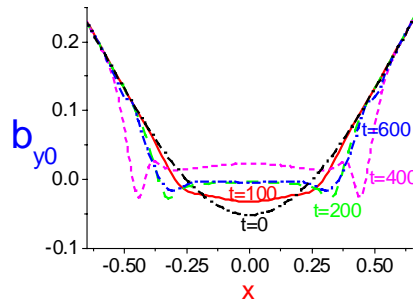


Fig. 3, Profiles of  $B_{y0}$  at  $t=0, 50, 100, 200, 400,$  and  $600$ .

In order to study the velocity layer formation in development of resistivity induced tearing modes, the electron viscosity is neglected and the results are given in Figures 4 to 6 for  $x_s=0.25$ . Shown in Fig.~4 are the profiles of the poloidal velocity  $\bar{v}_y(x)$  for the magnetic Reynolds number  $S=10^2$  (the line in black),  $10^3$  (the line in purple),  $10^4$  (the line in blue), and  $10^5$  (the line in orange), respectively, at the instant of time when the peaks in the profiles reach maxima. (The overhead bars are omitted in the figure labels for simplicity.) The velocity fields are clearly shown being confined in the vicinity of the rational surfaces. The most notable changes appear at the boundaries of the velocity layers,

where the velocity fields become narrower and larger in amplitude as the magnetic Reynolds number  $S$  is increased from  $10^2$  to  $10^5$  which is still lower than the values for present tokamak plasmas. The amplitudes of the velocity may be estimated as  $v_y \sim 0.5v_A \sim 1.5 \times 10^7$  cm/s for a hydrogen plasma of poloidal magnetic field  $B_p=0.1$ T and density  $n=5 \times 10^{19}$  m $^{-3}$ . That is, it is comparable with the poloidal Alfvén velocity.

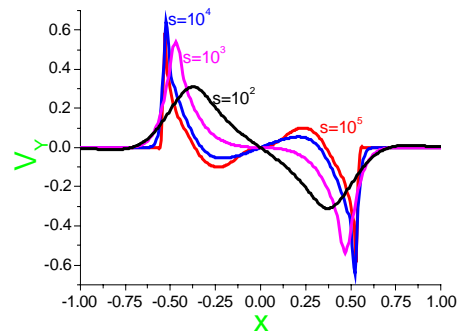


Fig.4, Profiles of the harmonic amplitude of the poloidal velocity.

In Fig.5 the profiles of the amplitude of velocity shear  $\partial \bar{v}_y / \partial x$ , (the lines with closed circles) contemporaneous with Fig.~1 are presented for (a)  $S=10^3$ , (b)  $S=10^4$ , and (c)  $S=10^5$ , respectively. The profiles of the amplitude of the perturbed radial magnetic field  $\bar{B}_x$  (the lines without symbols) are also shown for comparison.  $\bar{B}_x$  reaches the highest at the center of the reconnection region, decreases moving out and damped to zero at the locations of the magnetic island boundaries. The striking feature of the velocity shear profile is that it is concentrated in very narrow layers at the boundaries of the magnetic islands and is rather low inside and away from the islands. This indicates that the velocity shear layers exist not only in the development of electron viscosity induced double tearing mode but also in the resistivity induced mode.

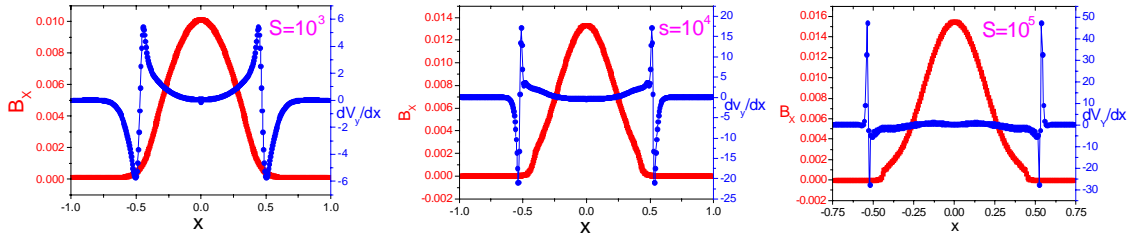


Fig.5 Profiles of the amplitudes of  $\partial \bar{v}_y / \partial x$  (the lines with closed circles) and  $\bar{B}_x$  (the lines without symbols) for (a)  $S=10^3$ , (b)  $S=10^4$ , and (c)  $S=10^5$ .

The time evolution of the peak velocity shear  $(v_y/dx)_{\max}$  (the blue dotted line) and the width of the magnetic island  $w_m$  (the black solid line) are given in Fig.~6(a) for  $S=10^6$ . The absolute values of  $w_m$  are estimated to be 0.6 cm at  $t=1800\tau_h$  if the radial scale length  $a=20$  cm is assumed. On the other hand, the peak of the velocity shear may be estimated as  $dv_y/dx \approx 6 \times 10^6/s$  at the same time slice for a hydrogen plasma of  $B_p=0.1T$ ,  $n=5 \times 10^{19}m^{-3}$  and  $a=20$  cm. This value is higher than typical growth rate of drift instabilities of  $\gamma_{dr} \approx \omega_{*e} \approx 10^5/s$  for plasma density gradient scale length  $L_n \sim 2$  cm.

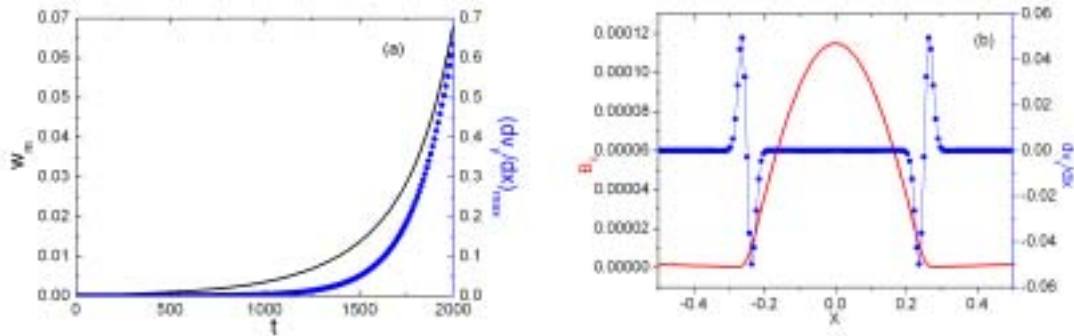


Fig. 6. (a) Time evolution of the peak velocity shear  $(v_y/dx)_{\max}$  (the blue dotted line) and the width of the magnetic island  $w_m$  (the black solid line). (b) Profiles of the amplitudes of  $\partial \bar{v}_y / \partial x$  (the blue line) and  $\bar{B}_x$  (the red line) for  $t=1800\tau_h$  for  $S=10^6$ .

In comparison with the profiles given in Fig. 5, where the velocity shear layers are approximately 0.25 away from the resonant surfaces located at  $\pm 0.25$ , the velocity layers in Fig. 6 are just located in the vicinities of the two resonant surfaces. The reason for such difference is that the mode is fully developed and the sizable magnetic islands ( $w_m \sim 0.5$ ) are formed in the case of Fig. 5 while the mode is in initial stage and the size of the magnetic islands is still very small ( $\sim 0.06$ ) in the case of Fig. 6. Therefore, it may be concluded that the velocity shear layers are located in the vicinities of the mode resonant surfaces in the initial stage of the mode development and move away from the surfaces, sticking to the boundaries of the magnetic islands, when the mode further develops and the magnetic islands grow.

#### 4. Conclusions and Discussion

The generation of a third kind flows, the MHD flows, in the development of double tearing modes mediated by electron viscosity as well as plasma resistivity in plasmas of reversed magnetic shear is clearly demonstrated. The strong sheared flows, driven by the magnetic energy released in the mode development, are in the poloidal direction and located at the magnetic island boundaries. Such flows certainly leads to strong  $\mathbf{E} \times \mathbf{B}$  sheared flows in the process of tearing mode development. The generated shear flows bear such striking qualitative similarity to the flows that accompany ITB formation (located in the proximity of low order rational surfaces, and just outside the magnetic islands). Quantitatively speaking, the magnitudes of the velocity and its shear were estimated as  $v_y \approx 1.5 \times 10^7$  cm/s and  $d v_y/dx \approx 6 \times 10^6$ /s, respectively, when the magnetic island width is as small as 0.6 cm for  $S=10^6$ . Such a shearing rate is higher than typical growth rate of drift instabilities of  $\gamma_{dr} \approx \omega_{*e} \approx 10^5$ /s for plasma density gradient scale length  $L_n \sim 2$  cm. The shearing rate is expected to be even higher in plasmas of typical tokamak parameters due to higher magnetic Reynolds number values. Therefore, this may provide a new physics understanding of how ITB trigger might be associated with low integer values of  $q$  in discharges of reversed magnetic shear and suggest that boundaries of an island represent transport barriers.

It has been pointed out that  $\mathbf{E} \times \mathbf{B}$  shear flow may be generated by a variety of mechanisms. The very stimulating observation that may provide supporting evidence for the new mechanism proposed in this work is that two radially separated ITBs simultaneously exist and follow the two  $q=2$  surfaces in a section of JET discharge pulse No. 51573 [1]. Moreover, it is confirmed that the ITBs are terminated by an  $m=2$  MHD mode which extends from the inner to the outer foot point location of the two ITBs. This is precisely the defining theoretical characteristic of the proposed double tearing mode. One of the most striking points of the experiments relevant to the model proposed in this work is that the onset of the double ITB structure exactly coincides with the onset of MHD activities that finally terminate the structure (See Fig.~8 of Ref.~1). These observations seem to support the thoughts proposed in this work.

ITBs occur under various conditions depending on interplay between mechanisms driving and suppressing plasma turbulence. The main driving mechanisms have been identified as gradients of plasma parameters such as density, velocity and temperature. Among

them, ion and electron temperature gradients are the most plausible candidates. The major suppressing mechanisms are magnetic shear and  $\mathbf{E} \times \mathbf{B}$  velocity shear. Therefore, ITB formation mechanism may be different under different discharge conditions due mainly to variation of generation mechanism of  $\mathbf{E} \times \mathbf{B}$  sheared velocity layer. The mechanism proposed in this work is relevant only in plasmas with non-monotonic  $q$  profiles and appropriate parameters. At this stage there is no unique nor universal mechanism. Further theoretical and experimental studies in more detail are certainly needed for full understanding of the mechanisms.

Since the fluctuation frequencies of the tearing modes and the spatial scale lengths are much lower and longer than that of the turbulence, the MHD flows studied in this work are expected to play a role in triggering of ITB formation. MHD flow layers at the boundaries of the magnetic islands have been observed in helical device LHD [7] and are anticipated and worthwhile for further studies in tokamak experiments.

**Acknowledgements** This work is supported by the National Natural Science Foundation of China, Grant Nos. 10575031 and 10575032.

## References

- [1] Jofrrin E, Challis C D, Conway G D *et al.* 2003 Nucl. Fusion, **43** 1167 and the references therein.
- [2] Jofrrin E, Gorini G, Challis C D *et al.* 2002 Plasma Phys. Control. Fusion **44** 1739.
- [3] Wolf R C 2003 Plasma Phys. Controlled Fusion **45** R1.
- [4] Ishii Y, Azumi M, Kurita G, and Tuda T 2000 Phys. Plasmas **7** 4477.
- [5] Held E D, Leboeuf J N and Carreras B A 1999 Phys. Plasmas, **6**, 837.
- [6] Ichiguchi K and B. A. Carreras 2004 EPS.
- [7] Ida K *et al.* 2002 Phys. Rev. Lett. **88**, 015002.
- [8] Dong J Q, Mahajan S M, Horton W, 2003 Phys. Plasmas **10** 3151.
- [9] Dong J Q, Mou Z Z, Long Y X, Mahajan S M 2004 Phys. Plasmas **11** 5673.